Difference Spatial Distribution Function Analysis of Methanol and Ethanol Solutions

Toshiyuki HATA and Yukio ONO*

Faculty of Pharmacy and Pharmaceutical Sciences, Fukuyama University, Sanzo, Gakuen-cho, Fukuyama, Hiroshima 729–0292, Japan. Received November 24, 1998; accepted February 22, 1999

Spatial distribution functions (SDFs), $g_{OO}(x,y,z)$ and $g_{OH}(x,y,z)$, which show the probability of atom–atom pair distribution between solute and solvent atoms, have been used to characterize the anisotropic structure of solutions in computer simulations. In this article, a new method for structural change analysis is proposed based on the difference spatial distribution function (DSDF) $\Delta g_{OO}(x,y,z)$, and is applied to liquid water, and to infinitely dilute aqueous solutions of methanol and ethanol. Based on the results of SDF in methanol and ethanol solutions, the distribution of solvent water can be classified into three groups: hydrogen acceptor, hydrogen donor, and hydrophobic hydration regions. Regarding the effect of hydrophobic groups, the DSDF (*i.e.* $\Delta g_{OO}(x,y,z)=g_{OO}(x,y,z)_{EtOH}-g_{OO}(x,y,z)_{MeOH}$) results indicated that the distribution volume of hydration water surrounding the alcohol molecule in the hydrogen acceptor region decreases with increasing steric bulk of the hydrophobic group. However, binding energy in this region is stabilized by an increase in the coordination number. Moreover, from the results of DSDF at 298 and 273 K (*i.e.* $\Delta g_{OO}(x,y,z,\Delta T)=g_{OO}(x,y,z,298\,K)-g_{OO}(x,y,z,273\,K)$), the distribution of hydration water spreads out over the region surrounding the hydrogen acceptor and donor. This result is reasonable since an increase in the fluctuation of the network structure results from a rise in temperature. The new DSDF method presented in this work should be widely applicable to structural change analysis of hydration structure for anisotropic solutions by computer simulation.

Key words aqueous alcohol solution; spatial distribution function; difference spatial distribution function; hydration structural change; Monte Carlo simulation

Theoretical evaluation of the effect of environment on the physico-chemical properties of bioactive substances and drugs is essential to the understanding of chemical and biological reactions in solution. In order to elucidate the structural geometries and physico-chemical properties of these molecules in solution, various theoretical techniques, such as molecular orbital methods and molecular mechanics, have been used. Because only solute molecules, and not solvent are characterized by these methods, new approaches to understand solvent effect have been developed by numerous investigators.[1—3] The main approach is reaction field theory[4] in which solute molecule interacts with a continuous medium characterized by a dielectric constant ε. This dielectric continuum model, in various forms, has been successfully applied to the problem of solvent effect. However, experimental determinations of radial distribution functions (RDFs), obtained using X-ray[5] and neutron diffraction[6] methods in liquid water, have indicated that the local structure of short-range order water molecules surrounding the central water molecules are in a tetrahedral structure, and not a homogeneous continuum structure. These experimental results show that solvent effect is not reliably estimated by the dielectric continuum model, assuming a homogeneous continuum structure for solvent surrounding the solute molecule. On the other hand, Monte Carlo (MC) and molecular dynamics (MD) methods are free from such approximations. In practice, however, application of these methods to the investigation of the hydration structure for a large molecular system requires a prohibitive amount of time.

Liu and Brady have employed spatial distribution functions (SDFs) to analyze three-dimensional local structure in aqueous sugar solutions,[7] as well as in liquid water[8] and methanol solution by Svishchev and his co-workers.[9] This SDF technique is very effective for visualizing the three-dimensional anisotropic structure in liquid and solution, but the RDF technique can only be projected to a one-dimensional distribution.

Based on these restrictions, our major goal is to develop a new method for the evaluation of solvent effects by considering the local structure of solvent water on the basis of the SDF technique. With regards to bioactive substances containing hydrophobic and hydrophilic groups, we can employ this technique to analyze the effects of amphoteric solute molecules. In the present investigation, we examined methanol and ethanol as simple model compounds. Infinitely dilute aqueous solutions of methanol and ethanol are hereafter referred to as methanol and ethanol solutions, respectively.

This paper describes the following results. First, by using SDF calculated by MC simulation, we characterize the hydration structure in methanol and ethanol solutions. Second, since the steric bulk of the hydrophobic group affects the hydration structure, this effect is examined using the results of difference SDF (DSDF). This is important since it is well known that enzymatic reactions have an optimum temperature, and structural changes in solvent water caused by temperature change are considered to particularly affect such reactions *in vivo*. Third, hydration structural changes occurring in conjunction with the temperature changes are described.

Computational Procedure

Monte Carlo Simulation MC simulations were carried out within the Metropolis scheme[10] in NVT ensemble. The number of molecules adopted in this calculation was 216 water molecules for liquid water and one methanol (or ethanol)+215 water molecules for alcohol solutions. The temperatures of all systems were 298 and 273 K. The molar volume employed was 18.015 $cm^3\,mol^{-1}$, obtained from 1.0 g cm^{-3} as the density of liquid water, and this corresponds to a

* To whom correspondence should be addressed.

cube with a cell length of 18.63 Å. Thus, all systems were assumed to describe a cube of equal volume.

SPC potential[11] and TIPS potential[12] functions were employed to represent intermolecular interactions for water and alcohols, respectively. Intermolecular interactions are described using Coulomb and Lennard-Jones terms as:

$$\Delta E=\sum_{i}^{\text{in}\,A}\sum_{j}^{\text{in}\,B}(q_i q_j e^2 r_{ij}+A_{ij}/r_{ij}^{12}-C_{ij}/r_{ij}^{6})$$

The coefficients, A_{ij} and C_{ij}, are obtained from $\sqrt{A_{ii}\times A_{jj}}$ and $\sqrt{C_{ii}\times C_{jj}}$, respectively. The following geometries were used in this investigation. Interatomic distance and bond angle for water: r(OH)=1.0 Å and ∠HOH=109.47°. The corresponding values for methanol and ethanol were r(OH)=0.945 Å, r(CO)=1.430 Å, r(CC$_O$)=1.512 Å, ∠COH=108.5° and ∠CCO=107.8°. The C–C–O–H dihedral angle for ethanol is 180.0°. These geometries were fixed in this MC simulation. All atoms containing water and alcohol molecules lie on the x–y plane. After excluding the first 750000 configurations, the subsequent 7500000 configurations were employed to obtain the statistical average in the present MC simulations.

Difference Spatial Distribution Function SDFs, which show the probability of atom–atom pair distribution between solute and solvent atoms, were used to characterize anisotropic solution structure in computer simulations. This function $g_{OO}(x,y,z)$ has the feature that it can easily characterize the three-dimensional structure of a solution.

Bosio *et al.*[13] reported for heavy water that the temperature dependence of the hydration structure can be determined by difference RDFs (DRDFs) obtained from X-ray diffraction at various temperatures, and that the tetrahedral structure of hydration water molecules increases with a fall in temperature. Therefore, in order to elucidate hydration structural change upon variation of temperature and the hydrophobic group, this DRDF technique was applied to SDF. The new function, where the DRDF technique is applied to SDF, is called the difference spatial distribution function (DSDF). These functions, which examine the effect of hydrophobic group and temperature dependence, are evaluated by means of the following equations, respectively.

$$\Delta g_{OO}(x,y,z)=g_{OO}(x,y,z)_{\text{EtOH}}-g_{OO}(x,y,z)_{\text{MeOH}}$$

$$\Delta g_{OO}(x,y,z,\Delta T)=g_{OO}(x,y,z,298\text{ K})-g_{OO}(x,y,z,273\text{ K})$$

Binding Energy Decomposition The binding energy (BE) can be calculated from the interaction energies between solute and the solvent molecules around it. The BE is evaluated from the summation of the product of SDF $g_{OO}(i,j,k)$ and averaged potential energies $\langle E(i,j,k)\rangle$ between the solute and solvent molecules in all spatial cells denoted by i, j, k. In the present study, the high density space is classified into three regions. First, the hydrogen acceptor (HA) region is distribution in the vicinity of the lone pair on the oxygen atom of the alcohol. Second, the hydrogen donor (HD) region is distribution in the direction of the hydrogen atom of the alcohol. Third, the hydrophobic hydration (HH) region is distribution around the alkyl group of the alcohol moiety. BE are calculated for each region using the equation below. For example, the value of BE for the HA region (subscript HA) is evaluated as:

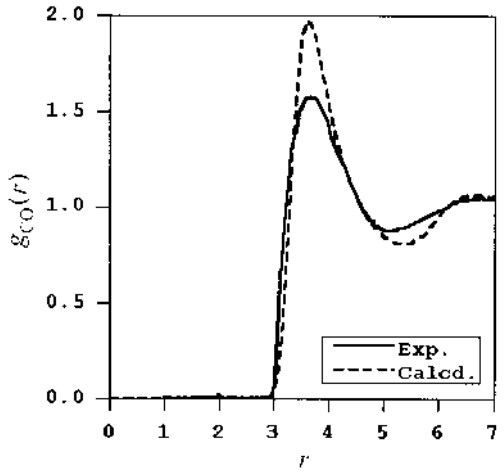

Fig. 1. Carbon (MeOH)–Oxygen (Water) RDF for Methanol Solution at 298 K from Neutron Diffraction Data and MC Simulation Data Using SPC and TIPS Potential Functions

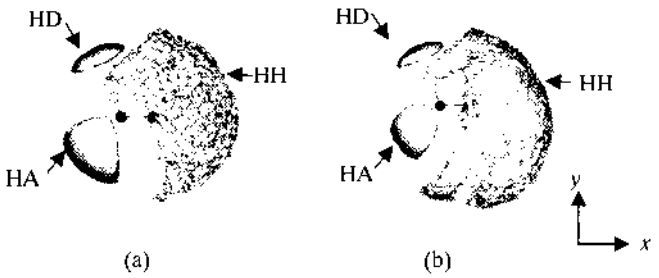

Fig. 2. Isosurface of Oxygen (Solute)–Oxygen (Water) SDF $g_{OO}(x,y,z)$=2.0 Viewed Down the z-Axis for (a) Methanol and (b) Ethanol Solutions at 298 K

The symbols HA, HD, and HH represent regions of hydrogen acceptor, hydrogen donor and hydrophobic hydration, respectively.

$$\langle BE\rangle_{\text{HA}}=\sum_{i,j,k\in\text{HA}}\frac{N}{V}\times\Delta V\times\langle E(i,j,k)\rangle\times g_{OO}(i,j,k)$$

Results and Discussion

Radial Distribution Function The utility of potential function can usually be examined by comparison of RDFs obtained from MC simulation and experiment. Figure 1 shows a RDF $g_{CO}(r)$ for a carbon(methanol)–oxygen(water) pair obtained by MC simulation (dotted line) and neutron diffraction results (solid line)[14] for methanol solution. As shown in Fig. 1, the theoretical prediction is in good agreement with the experimental result. This indicates that MC simulation employing SPC and TIPS potential functions is generally very suitable for the calculation of alcohol solutions.

Hydration Structure The hydration structure of methanol and ethanol can be analyzed by SDF $g_{OO}(x,y,z)$. The distribution of water molecules around methanol and ethanol is easily visualized by the graphic display technique method. Figure 2 shows the distribution of SDF $g_{OO}(x,y,z)$=2.0 between solute and water molecules as obtained from MC simulation at 298 K. As can be seen clearly, the high distribution of SDF can be classified into three regions: HA, HD, and HH. Except for the HD region, distribution of water molecules in methanol solution is clearly different from that in ethanol solution, according to the steric bulk of the hy-

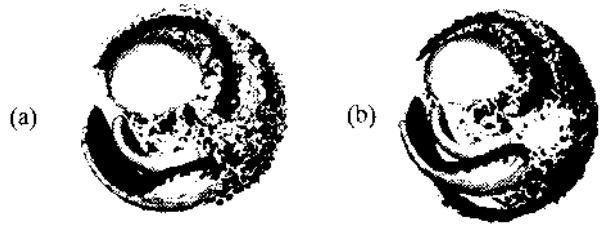

Fig. 3. Superposition Representation of Oxygen (Solute)–Oxygen (Water) and Oxygen (Solute)–Hydrogen (Water) SDF for (a) Methanol and (b) Ethanol Solutions at 298 K

The bright area shows oxygen–hydrogen distribution at $g_{OH}(x,y,z)=2.0$, and the dark area shows oxygen–oxygen distribution at $g_{OO}(x,y,z)=1.6$.

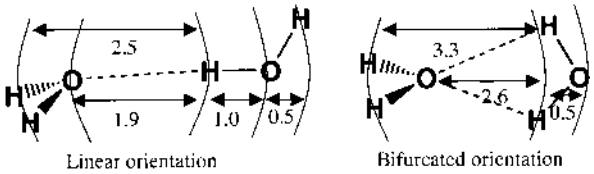

Chart 1. Water Dimer Structures Optimized by *ab initio* Molecular Orbital Calculations

Units for all interatomic distances are Å.

Table 1. Distribution Distances between Atoms of Solvent Water Molecules and of Central Molecule for Methanol Solution, Ethanol Solution, and Liquid Water

	HD		HA		
	O	H	H1	O	H2
Methanol solution	1.9	2.4	1.8	2.8	3.3
Ethanol solution	1.9	2.4	1.8	2.8	3.3
Liquid water	1.9	2.5	1.9	2.9	3.4

Units for all values are Å.

drophobic group (see next section).

With regards to the orientation of water molecules hydrogen-bonded with methanol and ethanol, two types of linear and bifurcated orientations can be considered. Okazaki *et al.*[15] investigated the hydration structure of methanol solution from the results of MC simulation, and reported that the main orientation of the water molecules was identical, with a linear orientation for the HD region and a bifurcated orientation for the HA region. Figure 3 shows a superposition of oxygen–oxygen and oxygen–hydrogen SDFs, $g_{OO}(x,y,z)$ and $g_{OH}(x,y,z)$, for methanol and ethanol solutions. Chart 1 shows linear and bifurcated structures optimized by MP2/6-31+G(2*d*, 1*p*) *ab initio* MO calculation, in which the geometry of the water molecule is fixed to the structure employed by the SPC potential function. Furthermore, maximum distribution locations in the first hydration shell shown in Fig. 2 were calculated by means of RDFs obtained from the MC simulation. The results of various distribution distances between solvent water atoms and the central molecule are summarized in Table 1 for the HA and HD regions.

In the HD region, the maximum distributions of oxygen and hydrogen atoms in water molecules occur at distance of approximately 1.9 and 2.4 Å from the hydrogen atom of the hydroxyl group in the alcohol molecule, respectively. This result coincides well with a linear orientation optimized by *ab initio* MO calculation (see Chart 1) and supports the result reported by Okazaki *et al.*

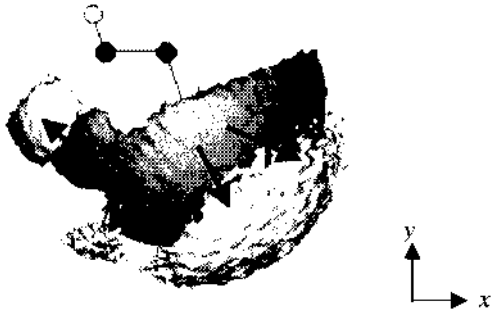

Fig. 4. Isosurface of Difference Oxygen–Oxygen SDF between Ethanol and Methanol Solutions Viewed Down the *z*-Axis

The bright area shows the increase of oxygen–oxygen distribution at $\Delta g_{OO}(x,y,z)=+1.0$, and the dark area shows the decrease of oxygen–oxygen distribution at $\Delta g_{OO}(x,y,z)=-1.0$.

In the HA region, however, the maximum distributions of hydrogen, oxygen and hydrogen atoms in water molecules occur at approximately 1.8, 2.8 and 3.3 Å from the oxygen atom of the alcohol molecules. Therefore, it is apparent that the triple layer structure is composed of each maximum distribution. As shown in Chart 1, maximum distributions of oxygen and hydrogen atoms of water molecules in a bifurcated orientation are considered to occur at approximately 2.6 and 3.1 Å. The double layer structure must be composed of each region. Taken together, these findings indicate clearly that the main spatial orientation of water molecules around the oxygen atom of the alcohol molecule supports a strongly linear orientation.

Effect of the Hydrophobic Group An isosurface of DSDF $\Delta g_{OO}(x,y,z)=\pm 1.0$ obtained from SDFs of ethanol and methanol solutions is shown in Fig. 4. This figure indicates that the distribution of hydration water molecules around the methyl group show a hemispheric decrease, and the decreased area is encircled by increased distribution of hydration water molecules around the ethyl group. On the other hand, hydration water molecules in the HA region are excluded by the steric bulk of the ethyl group, and are moved to the HD region side.

Applying the linked list clustering technique method,[16] the regions of SDF $g_{OO}(x,y,z)\geqq 2.0$ for oxygen–oxygen pairs are classified into three regions: HA, HD, and HH. Volume, coordination number (CN) and BE ($\langle BE\rangle_x$) for each region are given in Table 2.

The difference of hydration enthalpy ($\Delta\Delta H_h^0$) of ethanol and methanol solutions was calculated from the difference in their total BE, and the calculated values compared with experimentally observed values.[17] The coincidence of the calculated $\Delta\Delta H_h^0$ ($-6.95\,\mathrm{kJ\,mol^{-1}}$) in this work with the observed value ($-7.53\,\mathrm{kJ\,mol^{-1}}$) is satisfactory. On the other hand, the calculated $\Delta\Delta H_h^0$ obtained from the domain of SDF $g_{OO}(x,y,z)\geqq 2.0$ at 298 K, was $-4.58\,\mathrm{kJ\,mol^{-1}}$ (see Table 2). This $\Delta\Delta H_h^0$ is approximately *ca.* 66% of $\Delta\Delta H_h^0$ obtained from total BE. Therefore, the *BE* values ($\langle BE\rangle_x$) shown in Table 2 are considered to be widely applicable to investigation of hydration structure in solution.

In the HH region in methanol and ethanol solutions at 298 K, volume and CN values changed from 14.3 $\mathrm{Å^3}$ and 0.99 to

35.4 Å^3 and 2.52, and the results at 273 K were also similar to these mentioned above. These changes are considered to be due to the increase in solvent accessible surface area with a hydrophobic group.

As shown in Table 2, all values in the HD region in methanol solution are identical to those in ethanol solution. However, the volume (8.2 Å^3) in the HA region in methanol solution is greater than that (7.4 Å^3) in ethanol solution, whereas the CN (1.12) in the later are greater than that (1.03) in the former. On the other hand, $\langle BE\rangle_{HA}$ (-18.45 kJ mol^{-1}) in methanol solution is greater than that (-20.24 kJ mol^{-1}) in ethanol solution. Taken together, these results indicate that the contribution of stability to $\langle BE\rangle_{HA}$ is not influenced by the decreased volume in ethanol solution, because the density of hydration water molecules is increasing in the HA region.

Table 2. Results of Volume, CN, and BE Decomposition for Methanol and Ethanol Solutions at 298 and 273K

	Methanol			Ethanol		
	Volume	CN	$\langle BE\rangle_x$	Volume	CN	$\langle BE\rangle_x$
298K						
HA	8.2	1.03	−18.45	7.4	1.12	−20.24
HD	3.3	0.66	−9.36	3.3	0.67	−9.67
HH	14.3	0.99	−1.65	35.4	2.52	−4.13
Sum	25.8	2.68	−29.46	46.1	4.31	−34.04
273K						
HA	7.8	1.08	−19.55	7.3	1.20	−22.15
HD	3.1	0.71	−10.36	3.2	0.71	−10.22
HH	18.0	1.27	−1.88	40.8	2.94	−5.00
Sum	28.9	3.06	−31.79	51.3	4.85	−37.37

Units for volumes and $\langle BE\rangle_x$ are Å^3 and kJ mol^{-1}, respectively. Subscript x on $\langle BE\rangle_x$ indicates HA, HD, and HH.

Contour maps of the BE and SDF $g_{OO}(x,y,z)$ distributions on the x–y plane of $z=0.075$ Å are shown in Fig. 5. SDF distribution contour maps (right column) indicate clearly that the extent of oxygen atom distribution in the HD region centered at $x=-1.0$ Å and $y=2.6$ Å in methanol solution is the same as that in ethanol solution. However, the extent of oxygen atom distribution in the HA region in ethanol solution decreases appreciably relative to that in methanol solution. In the HH region, the distribution of the former increases compared to that of the latter. For example, the maximum distribution of an oxygen atom in the HA region is the central position at $x=-1.7$ Å and $y=-2.2$ Å in ethanol solution, and at $x=-1.4$ Å and $y=-2.2$ Å in methanol solution. The extent of distribution in the former narrows obviously relative to that in the latter, and the position shifts to the opposite direction of the hydrophobic group. On the other hand, BE contour maps (left column) indicate that BE distribution for the vicinity centered at $x=0.0$ Å and $y=-3.7$ Å in ethanol solution change from negative values in methanol solution to positive ones in ethanol solution. This means that the stable BE distribution area in the HA region decreases in ethanol solution. Taken together, these results clearly indicate that this change is due to enhanced repulsive area for the HH region.

Effect of Temperature Change As shown in Table 2,

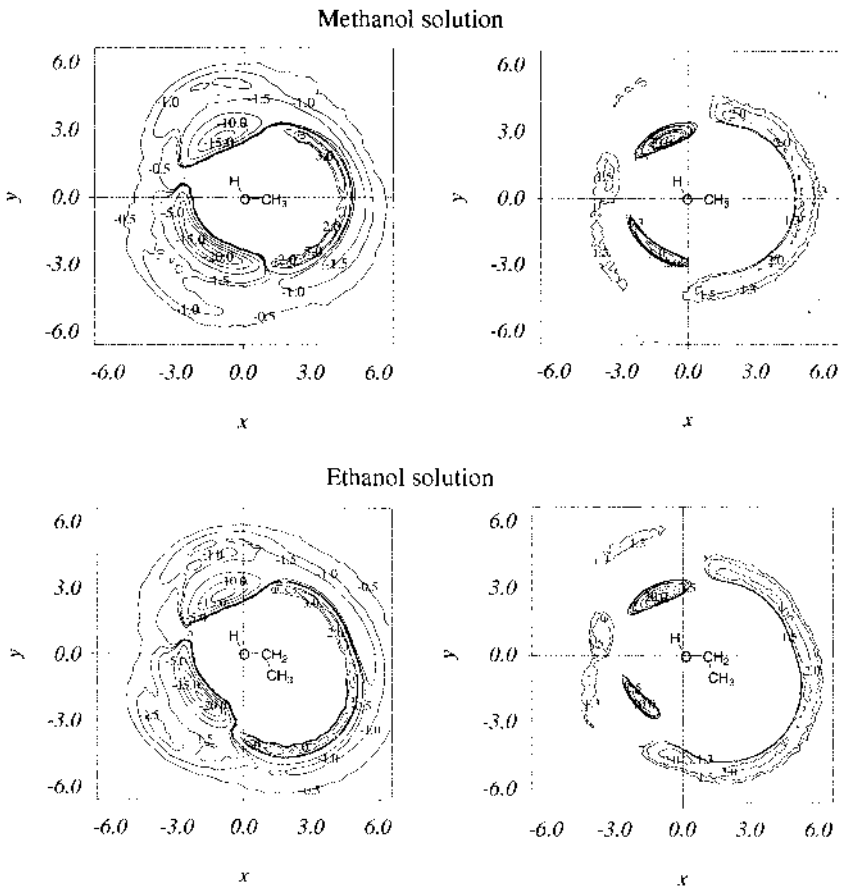

Fig. 5. Contour Maps of Binding Energies and Oxygen–Oxygen Distributions for Methanol and Ethanol Solutions at 298 K

The contour map at the left shows the binding energies and that at the right shows oxygen–oxygen distributions.

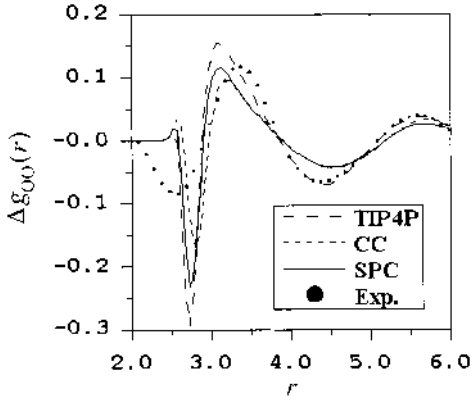

Fig. 6. Difference Oxygen–Oxygen RDF between RDFs at 273 and 298 K for Liquid Water

Table 3. Results of Difference CN (ΔCN) between Area Under Curves at 298 and 273 K

	1		2		3		4	
	ΔCN	r/Å	ΔCN	r/Å	ΔCN	r/Å	ΔCN	r/Å
Methanol	$<+0.01$	2.5	-0.11	2.8	$+0.19$	3.4	-0.16	4.6
Ethanol	$<+0.01$	2.6	-0.11	2.8	$+0.20$	3.2	-0.14	4.6
Liquid water	$+0.01$	2.5	-0.13	2.8	$+0.27$	3.1	-0.30	4.5

The values r show maximum and minimum peak positions obtained from DRDFs. Methanol and ethanol are methanol and ethanol solutions.

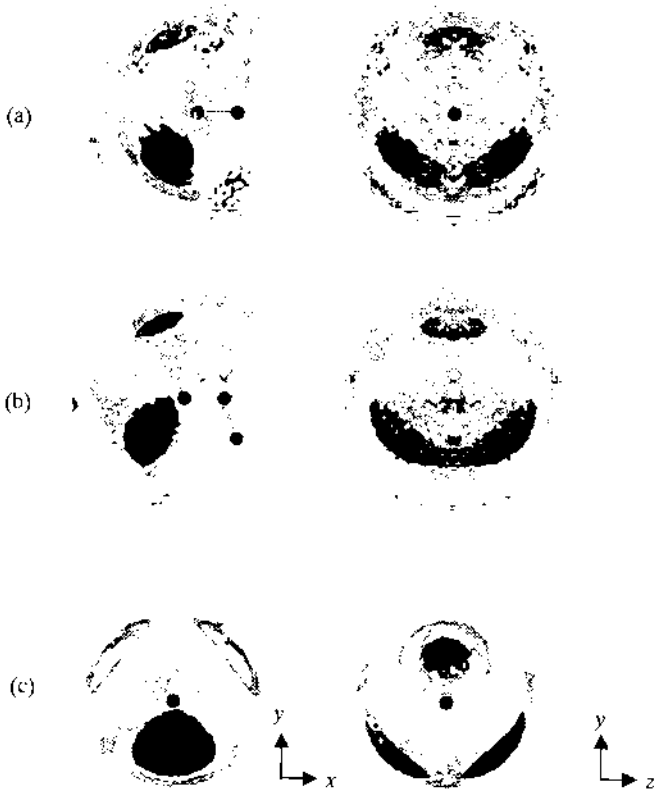

Fig. 7. Difference Oxygen–Oxygen SDF between SDFs at 273 and 298 K for (a) Methanol Solution, (b) Ethanol Solution, and (c) Liquid Water

The bright area shows the increase in the oxygen–oxygen distribution and the dark area shows the decrease in the distribution. The isosurface of $\Delta g_{OO}(x,y,z)=\pm 0.25$ for alcohol solutions and $\Delta g_{OO}(x,y,z)=\pm 0.15$ for liquid water are shown. Left and right columns are isosurface viewed down the z-axis and x-axis, respectively.

the volume in the hydrogen bond (HA and HD) regions increase with a rise in temperature, while that of the HH regions decrease. Although all CN values in the hydrogen bond and hydrophobic regions, and the contribution of stability to $\langle BE \rangle_x$, decrease with a rise in temperature, these results indicate that only the volume is influenced differently by the temperature change.

Bosio *et al.*[13] reported that DRDF obtained from the isochoric temperature difference of the X-ray structure factor increased with a fall in temperature, and led to a tendency to build up a tetrahedral network. Figure 6 shows the DRDFs $\Delta g_{OO}(r, \Delta T)$ at 298 and 273 K calculated by the present MC simulation using the SPC potential function (solid line) and the experimental results at 296.65 and 273.17 K measured by Bosio *et al.* (dotted line) for liquid water. The first negative peak calculated by the present work is clearly deeper than that in the experimental results. However, the positions of this peak and the intensities of the other peaks coincide approximately with those determined experimentally. The results calculated by CC potential fuction[18] and TIP4P potential function[19] are also similar to those mentioned above. The DRDFs $\Delta g_{OO}(r, \Delta T)$ for methanol and ethanol solutions are also similar to those for liquid water.

Table 3 shows maximum and minimum peak positions obtained from the DRDFs for alcohol solutions and liquid water, and the variation of CN values (ΔCN) in the area under the curve at each peak. All peak positions for alcohol solutions are in fair agreement with those for liquid water. The ΔCN values of the first and second peaks for methanol and ethanol solutions are the same as those for liquid water, while the ΔCN values of the third and fourth peaks for the former are different from those of the latter. It is well known that the second and fourth peaks for liquid water correspond to the first and second hydration shells, respectively. Though the second peak (2.8 Å) for alcohol solutions corresponds to the first hydration shell, as does that for liquid water, the fourth peak (4.6 Å) for alcohol solutions is coordinated with the hydrophobic group moiety. The considerable variation of ΔCN for the fourth peak may be regarded as due to the difference in the hydration nature of liquid water and alcohol solutions.

Figure 7 shows the results of DSDF for liquid water, and methanol and ethanol solutions. A decreasing region of hydration water is observed in the distribution of both the HA and HD regions. An increasing region of hydration water is observed in the region surrounding the decreasing distribution in the HA and HD regions, and especially in the center of the HA region. As shown clearly in Fig. 7, these results suggest that fluctuation of the network structure formed by the hydrogen bond increases with a rise in temperature, and the distribution of hydration water spreads out over the region surrounding the HA and HD. Therefore, these results support the idea that this effect results in an increased distribution volume of hydration water in the HA and HD regions.

Conclusion

We have shown a new method for structural change analysis based on DSDF $\Delta g_{OO}(x,y,z)$ and described the results of characterization for the hydration structure of liquid water

and methanol and ethanol solutions by means of SDF $g_{OO}(x,y,z)$ and DSDF $\Delta g_{OO}(x,y,z)$.

From the results of the SDFs, $g_{OO}(x,y,z)$ and $g_{OH}(x,y,z)$, for alcohol solutions at 298 K, the distribution of hydration water can be divided into three regions, namely the HA, HD and HH regions. In particular, the spatial orientation of the hydrogen-bonded water is mainly the linear type.

The steric bulk of the hydrophobic group affects the distribution of hydration water in the HA region. The distribution in the HA region is attributed to repulsion between the hydrophobic group and solvent water, which is enhanced with increasing steric bulk of the hydrophobic group. However, as the CN in the HA region increases with increasing steric bulk, the binding energy of ethanol solution is stabilized in contrast to methanol solution.

From the results of DSDF $\Delta g_{OO}(x,y,z,\Delta T)$ obtained from SDFs $g_{OO}(x,y,z)$ at 298 and 273 K for methanol and ethanol solutions, it is apparent that the distribution of hydration water spreads out over the region surrounding the HA and HD. This observation is considered to be due to an increase in the fluctuation of the network structure of hydrogen bonds resulting from the rise in temperature.

It is expected that the new DSDF $\Delta g_{OO}(x,y,z)$ method presented in this work should be widely applicable to structural change analysis of anisotropic solutions by computer simulation. In order to investigate the influence of the steric bulk of hydrophobic groups on hydration structure in more detail, we are examining similar MC simulations for aqueous ether solutions.

References

1) Miertuš S., Scrocco E., Tomasi J., *Chem. Phys*., **55**, 117 (1981).
2) Hoshi H., Sakurai M., Inoue Y., Chûjô R., *J. Chem. Phys*., **87**, 1107 (1987).
3) Klanmt A., Schüürmann G., *J. Chem. Soc*., *Perkin Trans. 2*, **1993**, 799.
4) Still W. C., Tempczyk A., Hawley R. C., Hendrickson T., *J. Am. Chem. Soc.*, **112**, 6127 (1990).
5) Narten A. H., Danford M. D., Levy H. A., *Discuss. Faraday Soc*., **43**, 97 (1967).
6) Soper A. K., Phillips M. G., *Chem. Phys*., **107**, 47 (1986).
7) Liu Q., Brady J. W., *J. Am. Chem. Soc*., **118**, 12276 (1996).
8) *a*) Svishchev I. M., Kusalik P. G., *J. Chem. Phys*., **99**, 3049 (1993); *b*) Kusalik P. G., Svishchev I. M., *Science*, **265** 1219 (1994); *c*) Svishchev I. M., Kusalik P. G., *J. Chem. Phys*., **100**, 5165 (1994).
9) Laaksonen A., Kusalik P. G., Svishchev I. M., *J. Phys. Chem. A*, **101**, 5910 (1997).
10) Metropolis N., Rosenbluth A. W., Rosenbluth M. N., Teller A. H., Teller E., *J. Chem. Phys*., **21**, 1087 (1953).
11) Berendsen H. J. C., Grigera J. R., Straatsma T. P., *J. Phys. Chem*., **91**, 6269 (1987).
12) Jorgensen W. L., *J. Am. Chem. Soc*., **103**, 355 (1981).
13) Bosio L., Chen S.-H., Teixeira J., *Phys. Rev. A,* **27**, 1468 (1983).
14) Soper A. K., Finney J. L., *Phys. Rev. Lett*.,**71**, 4346 (1993).
15) Okazaki S., Nakanishi K., Touhara H., *J. Chem. Phys.*, **78**, 454 (1983).
16) Ōsawa E., Gotō H., Hata T., Deretey E., *J. Mol. Struct*. (*Theochem.*), **398**—**399**, 229 (1997).
17) Franks F., "Water— a Comprehensive Treatise," Vol. 2, ed. by Franks F., Plenum Press, New York, 1972, Chapter 5.
18) Carravetta V., Clementi E., *J. Chem. Phys*., **81**, 2646 (1984).
19) Jorgensen W. L., Chandrasekhar J., Madura J. D., Impey R. W., Klein M. L., *J. Chem. Phys*., **79**, 926 (1983).